



## Exploiting optical properties of P3HT:PCBM films for organic solar cells with semitransparent anode

W.H. Lee<sup>a</sup>, S.Y. Chuang<sup>a</sup>, H.L. Chen<sup>a,\*</sup>, W.F. Su<sup>a</sup>, C.H. Lin<sup>b</sup>

<sup>a</sup> Department of Materials Science and Engineering, National Taiwan University, Taipei, Taiwan

<sup>b</sup> Institute of Electro-Optical Science and Engineering, National Cheng Kung University, Taiwan

### ARTICLE INFO

Available online 10 May 2010

#### Keywords:

Organic solar cell  
Optical thin film  
Semitransparent  
Thermal annealing

### ABSTRACT

In this study, we demonstrate optical properties of multilayer system in an organic solar cell based on poly (3-hexylthiophene) (P3HT) and 6,6-phenyl C61-butyric acid methyl ester (PCBM) with semitransparent anode through thermal annealing effect. The optical absorption is enhanced via optimizing annealing treatment which further elevates near-field electric field amplitude. The electric field amplitude at the interface (active layer/semitransparent anode) is enhanced after thermal annealing corresponding to effective absorption near to semitransparent anode. Moreover, the thickness of the active layer is optimized via optical thin-film model for enhancing the organic solar cell efficiency.

© 2010 Elsevier B.V. All rights reserved.

### 1. Introduction

For the advantages of the solution process, low-cost and compatible with flexible substrate, organic solar cells based on poly (3-hexylthiophene) (P3HT) and 6,6-phenyl C61-butyric acid methyl ester (PCBM) films have attracted much attention recently [1]. In organic solar cells, the Indium-Tin Oxide (ITO) film is used as a transparent electrode since it has high transmittance in visible region and ability of conduction. However, its resistance limits the efficiency in large area organic solar cells. Semi-transmission electrodes with low resistance are widely studied for organic light-emitting diodes [2,3]. Generally, the study of such anode is mainly focused on the far-field transmittance measured with a spectrometer and the value of sheet resistance. However, the transmittance of semitransparent film on the glass substrate is unequal to its real transmittance in the photovoltaic device. Interference and interface reflection in multiple layers of a solar cell cause the loss of transmittance. For a multilayer structure, the optical property of each layer influences the light intensity in the active layer. The importance of optical interference for organic photovoltaic devices has been discussed previously [5–9]. With further study, activation of electromagnetic wave through the semitransparent electrode in the device such as interference and interface reflection can be simulated correctly by the optical thin-film theory with optical constants. Therefore, for optimizing parameters of the organic solar cell with semitransparent electrode, optical properties of each layer are considered as the substantial factor.

Recent study displayed that annealing processing influenced organic photovoltaic device efficiency significantly. Generally, it is believed that

annealing can improve the crystallization and orientation of polymer and found that the nano-scale phase separation occurred between polymer and fullerene after the thermal self-organization [4]. Under the thermal annealing processing, the refractive index ( $n$ ) and extinction coefficient ( $k$ ) of the active layer varies with distinct temperature. Through the optical constant variation, optical property of the multilayer system with semitransparent anode is stated in near-field analysis. Appropriate optical property is the main reason for choosing gold as the semitransparent electrode. The intrinsic transmittance peak (ca. 510 nm) of a gold film matches the absorption peak of the P3HT:PCBM film (ca. 530 nm). The sheet resistance of the gold film is ca.  $1 \Omega/\text{cm}^2$  as thickness of 20 nm that is far less than an ITO film has sheet resistance of about  $20 \Omega/\text{cm}^2$ . With each layer optical constant acquired, the actual absorption in the active layer is calculated in the multilayer system. Because the enhancement in optical absorption was not sufficient to explain this unproportional increase of the solar cell efficiency [10], the detailed study of the active layer must be examined. Only charges dissociated in the active layer being collected by electrodes can contribute to the solar cell efficiency. The recombination in the bulk active layer limits the power conversion rate [11]. The investigation of electric field of incident light distribution at the interfaces of the organic thin film directly indicates the efficient absorption of electromagnetic wave. Therefore, we optimized the organic photovoltaic device parameters considering effective absorption.

### 2. Experimental details

Borosilicate crown glass (BK-7) substrates were cleaned in an ultrasonic bath by using acetone and isopropanol then rinsed with deionized water and dried with nitrogen gas. For optical constant measurement, organic thin films were spun on substrates. Bulk heterojunction polymers

\* Corresponding author.

E-mail address: [hsuenlichen@ntu.edu.tw](mailto:hsuenlichen@ntu.edu.tw) (H.L. Chen).

were prepared from a solution dissolved in chlorobenzene (CB) (Sigma Aldrich) of P3HT (Industrial Technology Research Institute, Taiwan) and PCBM (Aldrich Chemical) in 1:0.8 weight ratio. The samples were thermal annealed from room temperature to 60 °C, 80 °C, 100 °C, 120 °C, and 140 °C. All experimental processes were carried out in the glove box maintained at an atmosphere of less than 2.9 ppm O<sub>2</sub> and 0.1 ppm H<sub>2</sub>O. Optical constants (*n*, *k*) of each layer such as poly(3,4-ethylenedioxythiophene):poly(styrene sulfonate) (PEDOT:PSS) and organic layer were determined by ellipsometric and optical spectra measurements and then analyzed in optical thin-film model. Transmittance and reflectance of P3HT:PCBM film were measured using an optical spectrometer (Hitachi, U-4100).

For the measurement of photovoltaic device performance, the solar cells were fabricated under ambient conditions. The P3HT:PCBM thin film was spin-coated on gold thin-film coated glass substrates. A Cr film (3 nm) and a gold film (20 nm) were deposited on the substrate in the high vacuum chamber (~10<sup>-6</sup> Torr). The gold anode was spin-coated with PEDOT:PSS layer having a thickness of 30 nm. The PEDOT:PSS coated samples were then heated to 110 °C for 5 min. The active layer of the devices was coated from a solution of P3HT:PCBM at 1:0.8 weight ratio. Then the samples were moved to a high vacuum chamber (~10<sup>-6</sup> Torr), where an electrode of 100 nm aluminium was vapor deposited through a mask leaving active area of 4 mm<sup>2</sup>. After metal deposition, the samples were then thermal annealed in a glove box at 60 °C, 100 °C, and 120 °C, respectively. The organic photovoltaic device efficiency is measured under 100 W/m<sup>2</sup> simulated AM1.5 illuminations.

### 3. Results and discussion

Table 1 displays the current–voltage (*I*–*V*) curve of the photovoltaic device with distinct annealing temperature. The short circuit current density (*J*<sub>sc</sub>) was elevated significantly from 4.87 mA/cm<sup>2</sup> to 7.93 mA/cm<sup>2</sup> at the annealing temperature of 30 °C and 140 °C, respectively. Due to the P3HT:PCBM crystallization and ordered orientation, enhancement of the hole mobility and less electron–hole pair recombination occurs in the active layer. Therefore, with grading annealing temperature, the efficiency of the organic photovoltaic device increases substantially from 0.64% to 2.75%.

The curves in Fig. 1 display the transmittance and reflectance spectra of P3HT:PCBM blends on a glass substrate at various thermal annealing temperatures. The transmittance and reflectance reach their minimum leading to maximum absorption at 140 °C. The result displays that two vibronic peaks are much more pronounced in the film with higher annealing temperature. In addition, the peak of the higher temperature has red-shifts compared to the lower temperature ones. The red-shift may be assigned to a more flat molecular conformation and thus reduced torsion enabling a better intermolecular order [12]. In other words, these conformational chain defects (torsion, twists, or disruptions of planarity) can interrupt polymer conjugation and lead to a smaller *p*-conjugation length and blue shifting of the  $\pi$ – $\pi^*$  absorption band in linear conjugated polymers like P3HT.

From the reflectance, transmittance, and ellipsometric measurement, optical constants of P3HT:PCBM layer with various annealing

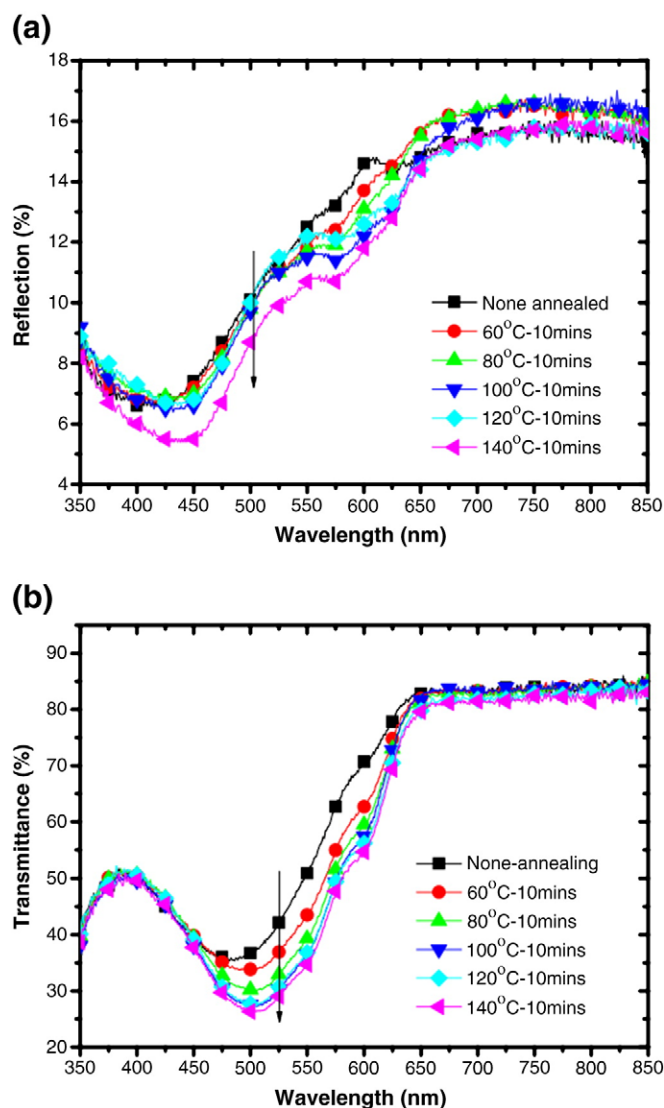


Fig. 1. The (a) reflectance and (b) transmittance spectra of P3HT:PCBM annealed at various temperatures for 10 min.

temperatures are displayed in Fig. 2. With grading temperature, the refractive index decreases as the extinction coefficient increases in the absorption region due to the abnormal dispersion phenomenon [13,14]. The extinction coefficient peak value ranging between 400 and 650 nm elevates with higher annealing temperature. The refractive index degrades from 2.03 to 1.81 and the extinction coefficient increases from 0.35 to 0.47 at 510 nm. The film annealed at 140 °C has the highest crystallinity as well as the maximum absorption coefficient ( $1.158 \times 10^7 \text{ m}^{-1}$ ). The thermal annealing process enhanced the crystallinity of P3HT due to the diffusion of PCBM molecules into aggregates. And the P3HT molecules crystallized in the PCBM free region. Larger extinction coefficient in the absorption band is caused by crystallization of the polymer material leading to more  $\pi$ – $\pi^*$  absorption. Moreover, X-ray diffraction measurement demonstrated that the annealing process is attributed to the conversion of P3HT/PCBM hybrid films to crystalline structure [13]. Strong correlation is observed between the crystallinity of the films and their optical absorption in the visible region.

As optical wave is propagating in a multilayer system, the reflectance at each interface, interference, and resonant effect in the cavity influence the efficiency of the organic photovoltaic device. For the optimization of external quantum efficiency of the organic solar

Table 1  
Properties of P3HT/PCBM-based photovoltaic devices prepared with various annealing temperatures.

Annealing temperature (°C)	V <sub>oc</sub> (V)	J <sub>sc</sub> (mA/cm <sup>2</sup> )	FF (%)	$\eta$ (%)
30	0.32	4.87	29.4	0.64
80	0.52	5.07	35.7	0.75
100	0.56	6.47	40.4	1.49
120	0.58	7.75	42.7	1.89
140	0.6	7.93	57.77	2.75

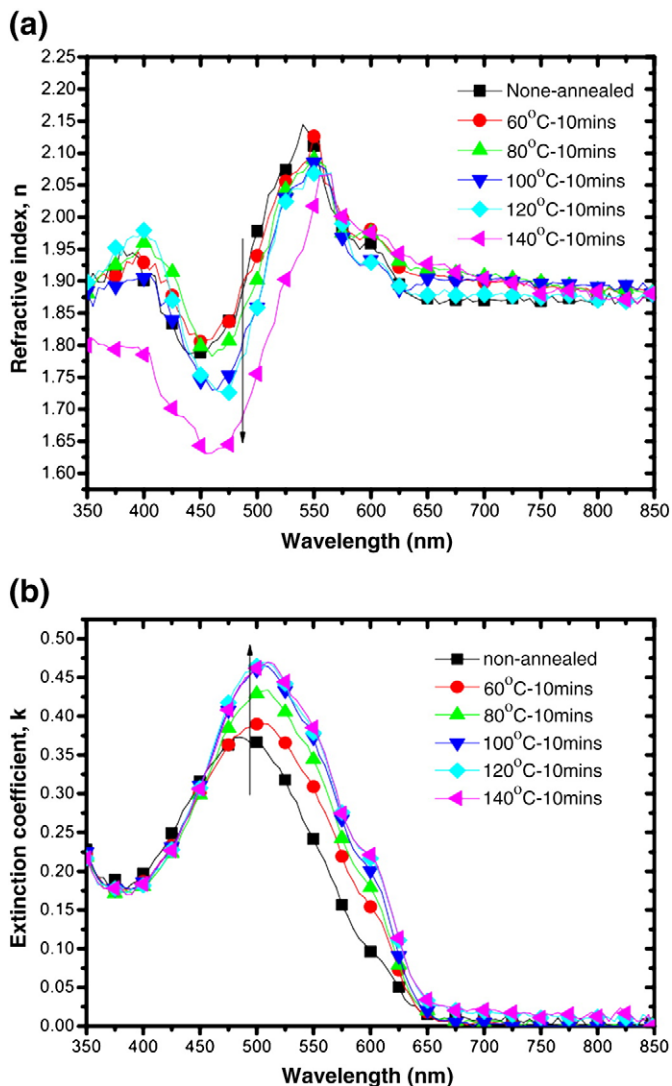


Fig. 2. The (a) refractive index and (b) extinction coefficient of P3HT:PCBM annealed at various temperatures obtained from spectrometric ellipsometry measurement.

cells, we obtained the optical constants of each layer including Au, PEDOT, P3HT:PCBM, and Al electrode. The structure of organic photovoltaic device used for calculation is glass substrate/Cr (3 nm)/Au (20 nm)/PEDOT (30 nm)/P3HT:PCBM (100 nm)/Al as displayed in Fig. 3. The light is incident into the glass substrate. The calculated absorption

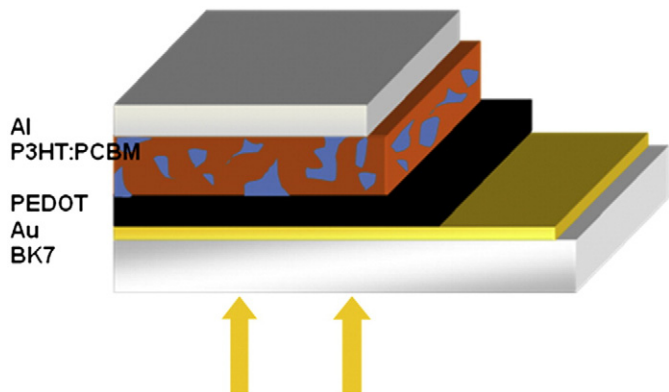


Fig. 3. The organic solar cell device structure with 20 nm thin gold film as semitransparent anode.

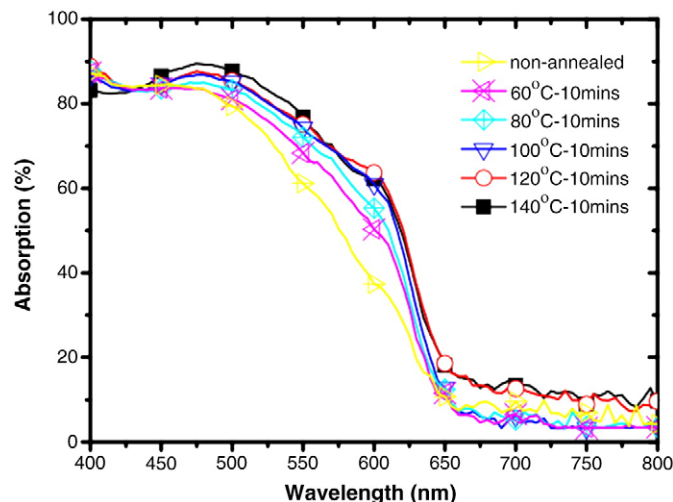


Fig. 4. The organic photovoltaic device absorption depending on the annealing temperature over a spectrum range of 400–800 nm.

spectra by optical thin-film model of the organic solar cell are displayed in Fig. 4. The result displays that the solar cell absorption reaches its maximum at 140 °C of annealing temperature. The enhancement of the absorption is due to the P3HT:PCBM crystallization and the reduction of interface reflection. The refractive index of PEDOT is 1.48–1.55 and 1.9 for P3HT:PCBM without any treatment at 510 nm. If the index difference ( $\Delta n = n_0 - n$ ) between interface can be reduced, the interfacial reflectance will decrease and more light will transmit to the under-layer. Due to the significant difference of refractive index, the interface between PEDOT and the organic layer has obvious reflectance. Since the refractive index of the organic thin film decreased as the annealing temperature elevates, the reflectance at the interface can be reduced. Therefore, the annealing process enhances the active layer absorption and reduces the interface reflectance at PEDOT/P3HT:PCBM simultaneously.

Due to the low mobility of carriers in the organic thin film, it is difficult for the carriers dissociated from the middle of the active layer to diffuse to the electrodes. Therefore, the electron–hole pairs dissociated in the active layer nearer to the electrode contribute to the effective absorption directly which corresponds to the more effective absorption of incident light. For electron–hole pairs generated in the middle of the active layer, electrons or holes must travel a long distance to reach electrodes which are mostly difficult. In contrast to carriers generated in the middle position, photo-generated carriers with short distance to electrodes can be collected effectively. Facilitating hole collection from donor towards device anode improves the photovoltaic response [15]. For P3HT:PCBM blend, annealing temperature [16], solvent [17], and regioregularity (RR) value [18] affect the mobility of electrons and holes. Generally, electrons own higher mobility than holes. Mihailetchi et al. displayed that the electron mobility of P3HT:PCBM after annealing 120 °C is ca.  $3 \times 10^{-7} \text{ m}^2 \text{ V}^{-1} \text{ S}^{-1}$  [16]. It is almost 20 times than the hole mobility of P3HT:PCBM. For the unequal mobility of electrons and holes, electron–hole pairs generated near the interface of PEDOT/P3HT:PCBM can conduct carriers effectively for solar cell performance.

With the grading change of annealing temperature, the electric field distribution of incident light in organic solar cell structure, glass/Cr (3 nm)/Au (20 nm)/PEDOT (30 nm)/P3HT:PCBM (100 nm)/Al (100 nm) is displayed in Fig. 5. The incident layer (Au) has the largest electric field amplitude. Degraded amplitude in PEDOT layer and elevated amplitude in the active layer are due to interference phenomenon in the device. The electric field amplitude at the interface of P3HT:PCBM/PEDOT elevates substantially from 0.41 to 0.58 as temperature increases to 140 °C. In the active layer, we focus on the region near the electrode where carriers can be collected effectively to the Au anode. In this region, large electric field amplitude could generate

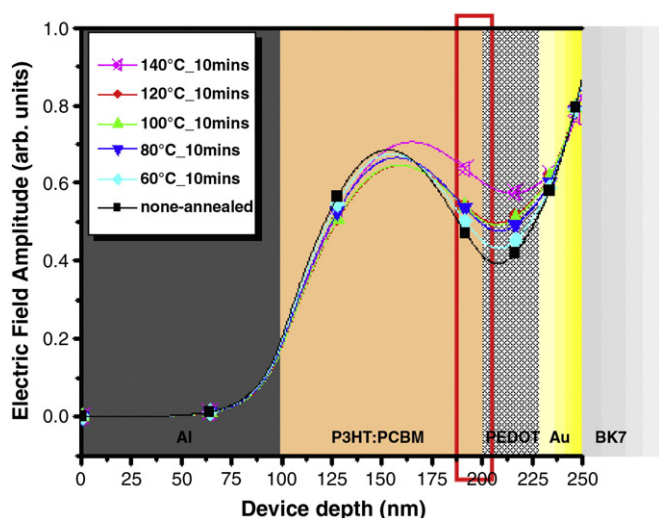


Fig. 5. The electric field amplitude distribution in the photovoltaic device with P3HT:PCBM thickness of 100 nm at distinct annealed temperature.

a lot of carriers that contribute to generate more electric current in the solar cell. The result displays that annealing process enhances the effective absorption due to more carriers dissociated at the active layer interface transport to the electrodes before recombination. The elevation of effective absorption results in higher power conversion efficiency. More than enhancement of electron–hole pair mobility, the

effective absorption near the electrodes and elevation of active layer absorption result in high efficiency.

For further optimization of the organic solar cell structure, the thickness of the active layer is discussed. Due to the interfacial reflectance and the interference, the electric field in the active layer varies dramatically with distinct active layer thickness. The finite-difference time-domain (FDTD) simulation for near-field analysis is applied at the wavelength of 510 nm corresponding to the P3HT:PCBM absorption peak. We used the FDTD method to analyze the propagation of light within the near-field regime of the organic solar cell device, glass/Cr (3 nm)/Au (20 nm)/PEDOT (30 nm)/P3HT:PCBM/Al(100 nm). The bright region indicates strong electric field amplitude while the dark region indicates weak electric field amplitude. Fig. 6(a) displays the electric field intensity of P3HT:PCBM layer having a thickness of 120 nm (annealed at 140 °C) indicating electric field is weak at the interface between the active layer and the semitransparent anode. Fig. 6(b) displays that the electric field is strong at the interface for the P3HT:PCBM layer having a thickness of 200 nm. Moreover, the electric field amplitude at the interface of the Au/active layer with various active layer thicknesses is displayed in Fig. 6(c). The electric field amplitude at the P3HT:PCBM/PEDOT interface varies with the distinct active layer. Electric field amplitude is significant at P3HT:PCBM films having a thickness of 80 nm and 200 nm.

4. Conclusions

In this study, we presented the optimized parameters including active layer thickness and thermal annealing process for P3HT:PCBM-based

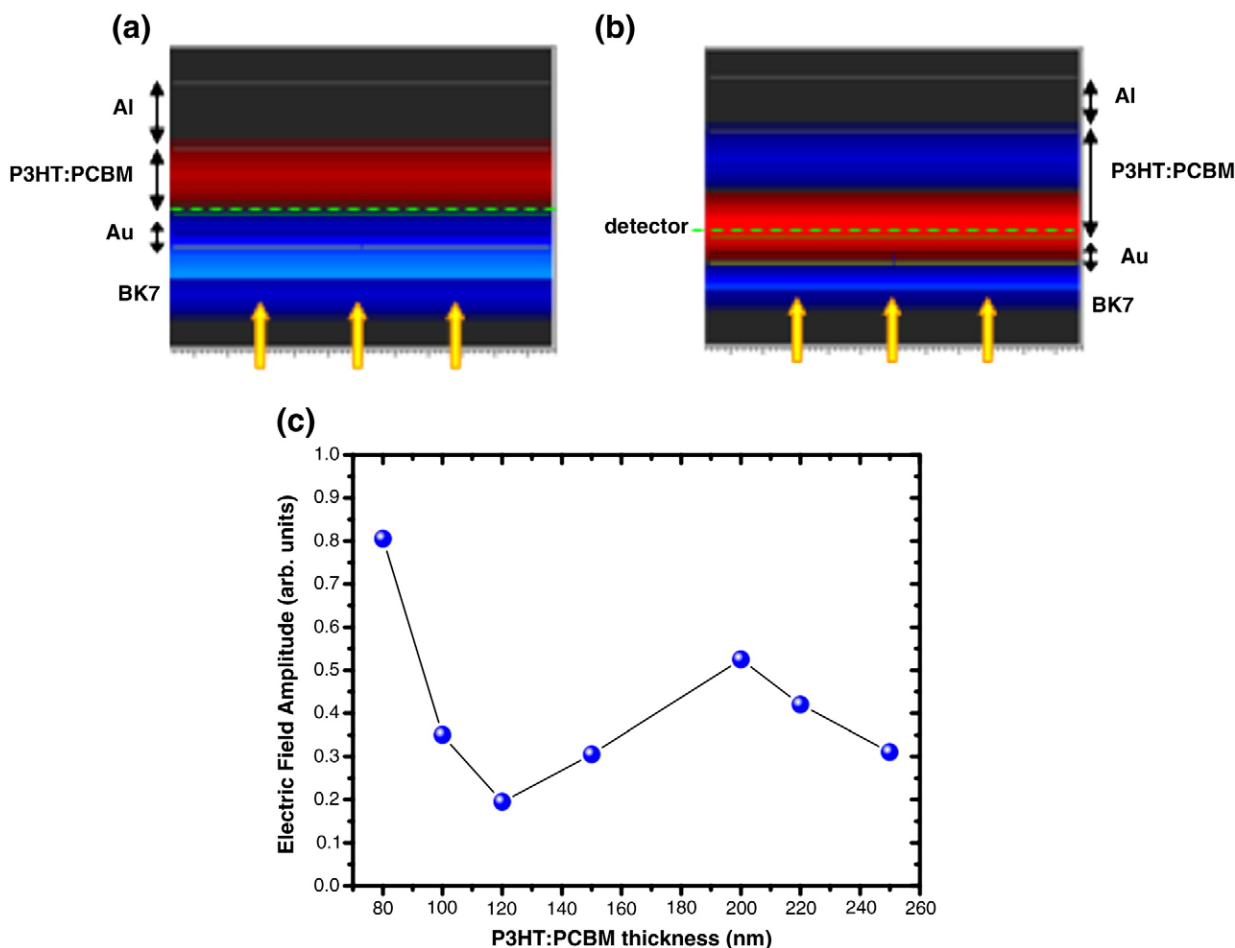


Fig. 6. FDTD simulation of electric field diagram in organic solar cell with P3HT:PCBM at (a) 120 nm and (b) 200 nm, and (c) electric field in P3HT:PCBM at two interfaces with various active layer thickness.

solar cells with thin gold film as the semitransparent anode. Optical constants of P3HT:PCBM films vary upon annealing temperature process. The degraded refractive index difference between P3HT:PCBM and PEDOT reduces the interfacial reflection. The upgraded extinction coefficient increases the optical wave absorption in the active layer. The photovoltaic device power conversion efficiency is elevated upon annealing process due to the enhancement of effective absorption because electron–hole pairs can be conducted effectively near the active layer and electrode interface. Via tuning the active layer thickness, the effective absorption of P3HT:PCBM can be optimized.

### Acknowledgement

The authors acknowledge the support from the National Science Council, Taiwan, R.O.C., under the project NSC-97-2221-E-002-046-MY3.

### References

- [1] C. Waldauf, P. Schilinsky, J. Hauch, C.J. Brabec, *Thin Solid Films* 451–452 (2004) 503.
- [2] H.J. Peng, X.L. Zhu, J.X. Sun, Z.L. Xie, S. Xie, M. Wong, H.S. Kwok, *Applied Physics Letters* 87 (2005) 173505.
- [3] G.M. Ng, E.L. Kietzke, T. Kietzke, L.W. Tan, P.K. Liew, F.R. Zhu, *Applied Physics Letters* 90 (2007) 103505.
- [4] D. Chirvase, J. Parisi, J.C. Hummelen, V. Dyakonov, *Nanotechnology* 15 (2004) 1317.
- [5] A.J. Moulé, J.B. Bonekamp, K. Meerholz, *J. Appl. Phys.* 100 (2006) 094503.
- [6] L.H. Slooff, S.C. Veenstra, J.M. Kroon, D.J.D. Moet, J. Sweelssen, M.M. Koetse, *Appl. Phys. Lett.* 90 (2007) 143506.
- [7] D.W. Sievers, V. Shrotriya, Y. Yang, *J. Appl. Phys.* 100 (2006) 114509.
- [8] N.K. Persson, O. Inganäs, *Sol. Energy Mater. Sol. Cells* 90 (2006) 3491.
- [9] L.A.A. Pettersson, L.S. Roman, O. Inganäs, *J. Appl. Phys.* 89 (2001) 5564.
- [10] H. Hoppe, N. Arnold, D. Meissner, N.S. Sariciftci, *Thin Solid Films* 451 (2004) 589.
- [11] G. Dennler, A.J. Mozer, G. Juska, A. Pivrikas, R. Osterbacka, A. Fuchsbaue, N.S. Sariciftci, *Org. Electron.* 7 (2006) 229.
- [12] Jean Roncali, *Chem. Rev.* 97 (1997) 173.
- [13] S.Y. Chuang, H.L. Chen, W.H. Lee, Y.C. Huang, W.F. Su, W.M. Jen, C.W. Chen, *J. Mater. Chem.* 19 (2009) 5554.
- [14] Grant R. Fowles, *Introduction to Modern Optics*, 2nd ed, Holt, Rinehart and Winston Press, New York, 1975.
- [15] S.W. Tong, C.F. Zhang, C.Y. Jiang, G. Liu, Q.D. Ling, E.T. Kang, D.S.H. Chan, C. Zhu, *Chem. Phys. Lett.* 453 (2008) 73.
- [16] V.D. Mihailetschi, H. Xie, B. Boer, L.J.A. Koster, P.W.M. Blom, *Adv. Funct. Mater.* 16 (2006) 699.
- [17] M. Morana, P. Koers, C. Waldauf, M. Koppe, D. Muehlbacher, P. Denk, M. Scharber, D. Waller, C. Brabec, *Adv. Funct. Mater.* 17 (2007) 3274.
- [18] Y. Kim, S. Cook, S.M. Tuladhar, S.A. Choulis, J. Nelson, J.R. Durrant, D.D.C. Bradley, M. Giles, I. McCulloch, C.S. Ha, M. Ree, *Nat. Mater.* 5 (2006) 197.